Application of 2-Deoxy-2-[18F]Fluoro-D-Galactose for Experimental Tumor Study

III. 14 Application of 2-Deoxy-2-[^{18}F]Fluoro-D-Galactose for Experimental Tumor study

Ishiwata K., Yamaguchi K.*, Kameyama N.**, Fukuda H.*, Tada M.*, Matsuzawa T.*, Muraishi K.**, Itoh J.**, Kawashima K., Takahashi T. and Ido T.
Cyclotron and Radioisotope Center, Tohoku University
Research Institute for Tuberculosis and Cancer, Tohoku University*
Institute of Brain Diseases, Tohoku University School of Medicine**

Fluorine-18 labeled 2-deoxy-2-fluoro-D-galactose ([^{18}F]FdGal) has been developed for measuring galactose metabolism in the liver with positron emission tomography (PET)[1-9]. The [^{18}F]FdGal is taken by the liver in the highest level, and is trapped in forms of 2-deoxy-2-[^{18}F]fluoro-D-galactose 1-phosphate ([^{18}F]FdGal-1-P) and UDP-2-deoxy-2-[^{18}F]fluoro-D-galactose (UDP-[^{18}F]FdGal). In this paper we apply the [^{18}F]FdGal for experimental tumor studies.

Materials and Methods

[^{18}F]FdGal was synthesized by the reaction of $CH_3COO^{18}F$ and tri-O-acetyl-D-galactal as described previously[3,7].

Donryu rats with hepatoma, AH109A and AH272, and with Yoshida sarcoma, YS, Wistar rats with glioma KEG-1 and C3H/He mice with mammary carcinoma, FM3A, were used.

Donryu rats with AH109A were injected with 30 μCi of [^{18}F]FdGal through a lateral tail vein. The rats were sacrificed at 10, 30, 60 and 120 min after injection. The tissue uptake was expressed as the differential absorption ratio (DAR), (counts of tissue/total injected counts) × (g body weight/g tissue), to correct the data for body weight of rats and mice.

For metabolic studies rats and mice were injected i.v. with [^{18}F]FdGal. The injected doses of [^{18}F]FdGal were 3 to 5 mCi and 0.6 to 1.5 mCi for rats and mice, respectively. The animals were sacrificed at 60 min after injection. The tumor uptake was measured as described as above. Analysis of metabolites was carried out by high-performance liquid chromatography (HPLC) as described in a previous paper[7].

Wistar rats bearing KEG-1 tumor were sacrificed at 60 min after i.v. injection of 5 mCi [^{18}F]FdGal. The frozen brain was cut into 40-um-thick slices. The slices were dried. An X-ray film** was exposed on these slices and then developed. Autoradiograms were scanned with a Chromoscan 3. The data were digitized and the density of radioactivity in the region of interest was measured.

Results

The results of tissue distribution of [^{18}F]FdGal in AH109A-bearing rats are represented in Fig. 1. The highest uptake was observed in the liver followed by the kidney and AH109A tumor. The radioactivity increased with time in the liver and AH109A. The uptake ratio of tumor to tissue increased with time, and the uptake ratios of tumor-to-brain, tumor-to-blood and tumor-to-muscle were 2.0, 4.4 and 15 at 60 min after injection.

In Table 1 the accumulation of [^{18}F]FdGal in five tumor tissues are summarized at 60 min after injection. To compare the data obtained from rats and mice, the uptake is corrected for body weight. Although the injected amounts of the [^{18}F]FdGal in the metabolic study were over 100 times higher than the amounts used in the tissue distribution study, a similar high uptake was measured in the AH109A tumor. KEG-1, FM3A and YS tumor tissues showed a slightly lower accumulation than AH109A and AH272. Fig. 2 shows a radio-HPLC chromatogram of metabolites in the acid-soluble fraction of AH109A tissue. Five components were detected. The [^{18}F]FdGal, the peak *a*, was eluted in a void volume of an anion-exchange column. The peaks *d* and *e* were identified to be [^{18}F]FdGal-1-P and UDP-[^{18}F]FdGal, respectively. The peaks *b* and *c* were not identified. In other four tumor lines the predominant metabolites were also [^{18}F]FdGal-1-P and UDP-[^{18}F]FdGal. The proportions of main three components are also represented in Table 1. The radioactivity in the acid-precipitable fraction was less than 1% of the total radioactivity in tumor tissue. In two hepatoma tissues the ratios of uridylate form were larger than in KEG-1, YS and FM3A tissues.

By autoradiography, the higher accumulation of radioactivity in KEG-1 tumor was clearly visualized from the surrounding brain tissue. Three cases are presented in Fig. 3. The relative density in several regions was expressed as the ratio to the normal cortex (Table 2). In the first case, Fig. 3A, the high density of ^{18}F was coincident with the regions deeply stained with hematoxylin and eosin, and the different regional distribution in the tumor was recognized. No accumulation of ^{18}F was shown in the central necrotic region. In other two cases without a necrotic region, the ununiformity of the ^{18}F distribution in tumor was also observed. In the normal brain tissue a different regional distribution was found. The cortex showed the highest density. The uptake ratios of tumor to cortex were 1.21 to 1.70.

Discussion

As indicated in the preliminary study using AH109A-bearing rats[8], in all tumors investigated the high uptake of radioactivity was observed. The metabolism of [^{18}F]FdGal results in the trapping of [^{18}F]FdGal as the phosphate and uridylate forms as observed in the liver and other tissues[7]. However, compared to the metabolism in the liver and brain, in the tumor

tissue the phosphate form is a predominant metabolite, and the proportion of UDP-[^{18}F]FdGal is much smaller. The metabolism of [^{18}F]FdGal is possibly due to the presence of galactokinase and UDP-glucose:galactose-1-phosphate uridyltransferase. The finding of minor metabolites indecates complicated metabolism of the [^{18}F]FdGal in tumor tissue compared to the liver tissue.

Among five tumors different characteristics were observed. Two hepatomas, AH109A and AH272, showed a slightly higher uptake than glioma, Yoshida sarcoma and mammary carcinoma. Also in these hepatomas the proportion of uridylate derivative was larger than in the other three tumors. These results may be explained as follows: the hepatoma has a high activity of galactose metabolism inherent in the host liver tissue. In the literature the galactokinase activity in Morris hepatoma was nearly equal compared with the activity in the host liver tissue, although both the concentration of UDP-galactose and the uridyltransferase activity were reduced to be a fourth to a half[10]. It could be possible that PET study using [^{18}F]FdGal differentiated the hepatoma from other kinds of tumors. This expectation was demonstrated by the preliminary PET study in patients with hepatocellular carcinoma[6]. On the other hand, the high uptake in KEG-1, FM3A and YS indicates that the [^{18}F]FdGal is also suitable for the imaging of tumors other than hepatoma, especially located in the regions of the head, neck and chest. The distinct regional distribution of radioactivity in KEG-1 by the autoradiography (Fig. 3A) represents the image of galactose metabolism rather than the breakdown of the blood-brain barrier.

In conclusion, because the metabolism of [^{18}F]FdGal in the tumor tissue results in the metabolic trapping of phosphate and uridylate forms, the combination of [^{18}F]FdGal with PET is promising for tumor imaging and has the potential to evaluate galactose metabolism in tumors.

References

1) Tada M., Matsuzawa T., Ohrui H. et al., Heterocycles 22 (1984)565.
2) Fukuda H., Matsuzawa T., Tada M. et al., Eur. J. Nucl. Med. 11 (1986) 444.
3) Tada M., Matsuzawa T., Yamaguchi K. et al., Conbohydr. Res. 161 (1987) 314.
4) Fukuda H., Yamaguchi K., Matsuzawa T. et al., Jpn. J. Nucl. Med. 24 (1987) 165.
5) Fukuda H., Yamaguchi K., Matsuzawa T. et al., Jpn. J. Nucl. Med. 28 (1987) 871.
6) Fukuda H., Yamaguchi K., Matsuzawa T. et al., J. Nucl. Med 28 (1987) 706 (Abstract).
7) Ishiwata K., Ido T., Imahori Y. et al., Nucl. Med. Biol. 15 (1988) 271.
8) Matsuzawa T., Fukuda H., Abe Y. et al., Proceedings of the International Symposium on Current and Future Aspects of Cancer Diagnosis with Positron Emission Tomography (PET 85) (1985) 1.

9) Fukuda H., Yamaguchi K., Matsuzawa T. et al., Proceedings of the International Symposium on Current and Future Aspects of Cancer Diagnosis with Positron Emission Tomography (PET 85) (1985) 24.
10) Reutter W., Bauer C. Adv. Exp. Med. Biol. 92 (1978) 405.

Table 1. Tumor accumulation and metabolites at 60 min after i.v. injection of 2-deoxy-2-[^{18}F]fluoro-D-galactose ([^{18}F]FdGal).

Tumor	No.	Uptake (DAR)	Metabolites* [^{18}F]FdGal (%)	[^{18}F]FdGal-1-P (%)	UDP-[^{18}F]FdGal (%)
AH109A	4	1.75 ± 0.12	7.2 ± 1.6	64.9 ± 2.1	17.4 ± 1.3
AH272	3	1.86 ± 0.21	7.2 ± 2.2	75.7 ± 3.6	14.8 ± 2.2
KEG-1	4	1.55 ± 0.41	9.4 ± 2.2	76.9 ± 3.6	9.1 ± 1.3$^{a,b'}$
YS	4	1.15 ± 0.30$^{b,b'}$	11.7 ± 4.1	80.5 ± 4.1	6.7 ± 3.8$^{a.b'}$
FM3A	3	1.40 ± 0.09$^{b,d'}$	3.0 ± 0.3	86.4 ± 1.2	9.4 ± 1.3$^{a,c'}$
Liver**			2.7 ± 0.1	36.4 ± 4.6	60.5 ± 3.2
Brain**			6.8 ± 0.5	76.9 ± 3.6	25.8 ± 0.6

*Percentage of each peak was normalized as total recoverd ^{18}F to be 100%.
**reference 7
Data indicate an average of three or four rats. Error is s.d.
A Students t-test was carried out: ^{a}P 0.001, ^{b}P 0.01(compared to AH109A), $^{b'}$P 0.01, $^{c'}$P 0.02, $^{d'}$P 0.05 (compared to AH272).

Table 2. Regional distribution of ^{18}F in brain section of rats with glioma, KEG-1, at 60 min after i.v. injection of 2-deoxy-2- [^{18}F] fluoro-D-galactose.

Region		Relative Density of ^{18}F*		
		Case A	Case C	Case D
1	Cortex	1.00	1.00	1.00
2	Striatum	0.80		0.84
3	Amygdaloid cortex		0.74	
4	Hippocampus		0.75	
5	Thalamus		0.95	
6	Hypothalamus		0.73	
7	Corpus callosum		0.74	
8	Tumor region	1.49	1.70	1.40
9	Tumor region	1.47	1.65	1.36
10	Tumor region	1.22	1.54	1.21

*The relative density in the individual region is presented as the density in the cortex, region 1, to be 1.00.

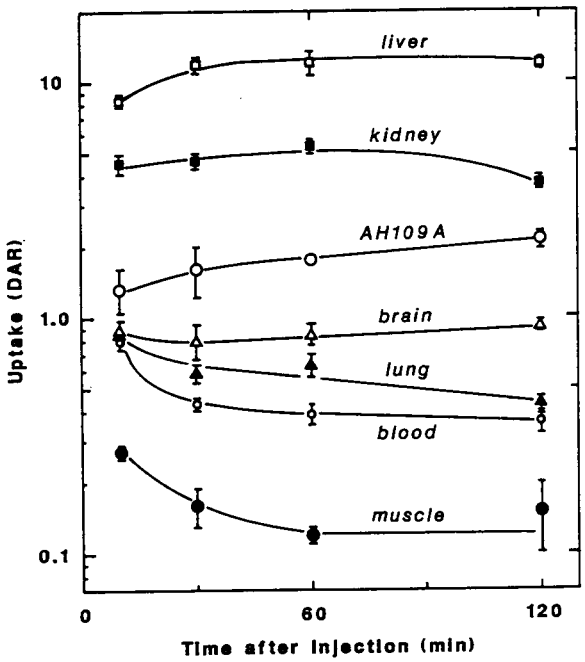

Fig. 1. Tissue distribution of ^{18}F after i.v. injection of 2-deoxy-2-[^{18}F]fluoro-D-galactose in rats bearing AH109A tumor.

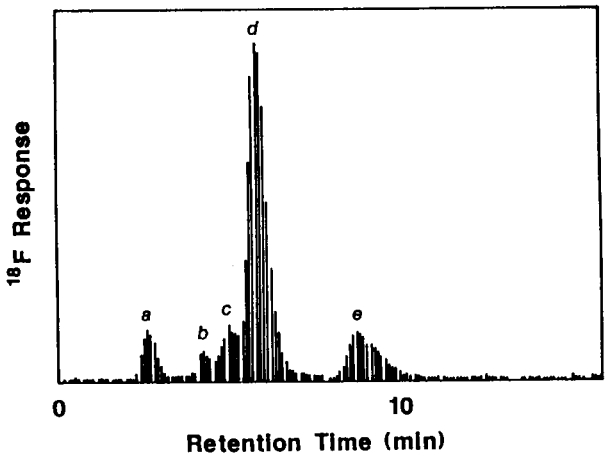

Fig. 2. High-performance liquid chromatography of ^{18}F-labeled metabolites in AH109A tumor tissue at 60 min after injection of 2-deoxy-2-[^{18}F]fluoro-D-galactose on a Radial-PAK SAX column. The peaks *a*, *d* and *e* are identified to be [^{18}F]FdGal, [^{18}F]FdGal-1-P and UDP-[^{18}F]FdGal, respectively[7].

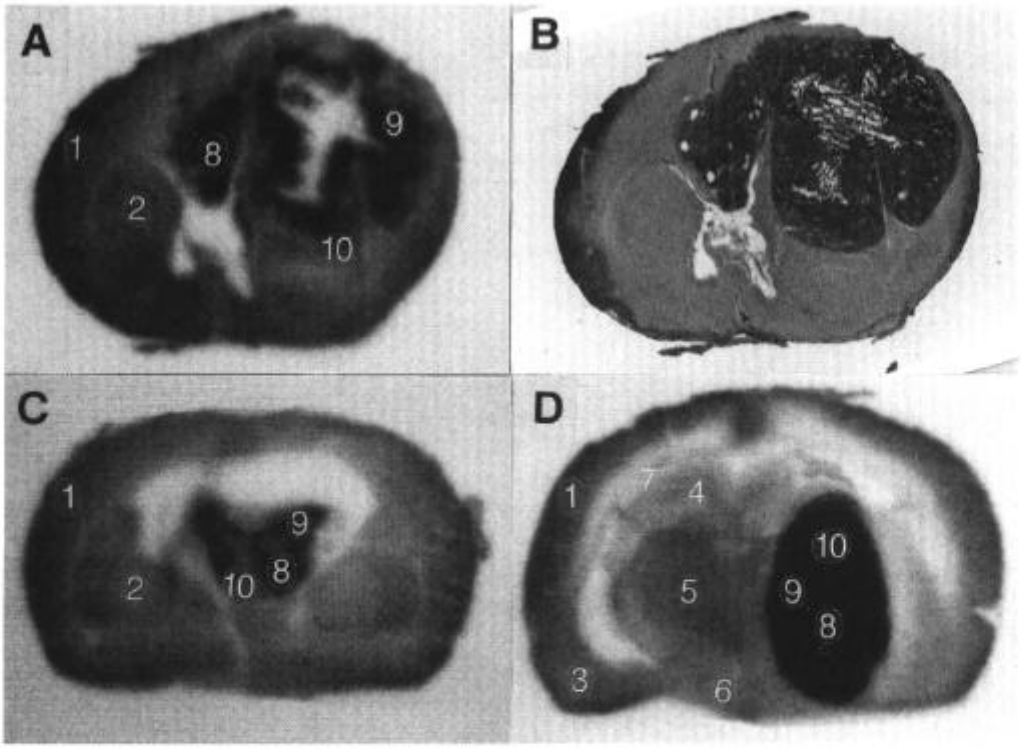

Fig. 3. Autoradiographic distribution of ^{18}F in the coronal section of rat brain with KEG-1 tumor after injection of 2-deoxy-2-[^{18}F]fluoro-D-galactose. Fig. 3A, 3C and 3D present autoradiograms of the individual rat. Fig. 3B presents the hematoxyline-eosin staining of the same brain section used to obtain the autoradiogram in 3A. The relative optical density in the egions 1 to 10 was measured, and the results are represented in Table 2.